

INFLUENCE OF Sb CONTENT ON PHASE COMPOSITION CHANGE OF NANOSCALED Co-Sb FILMS DEPOSITED ON HEATED SUBSTRATE

Yu. N. Makogon, E. P. Pavlova, S. I. Sidorenko, R. A. Shkarban

National Technical University of Ukraine “KPI”,
03056, Peremogy Avenue, 37, Kiev, Ukraine

y.makogon@kpi.ua, el_pavlova@inbox.ru, sidorenko@kpi.ua, haben@ukr.net

PACS 68.37.Ps, 68.55.Nq, 68.60.Dv, 73.50.Lw, 82.80.Yc, 84.60.Rb, 85.80.Fi

The subject of this study is the formation of the phase composition and structure in nanoscaled CoSb_x (30 nm) ($1.82 \leq x \leq 4.16$) films deposited by molecular-beam epitaxy on substrates of oxidized monocrystalline silicon at 200°C and the following thermal treatment in vacuum from $300\text{--}700^\circ\text{C}$. It is established that after deposition, the films are polycrystalline without texture. With increased Sb content, the formation of the phase composition in the films takes place in such a sequence as is provided by the phase diagram for the bulk state of the Co–Sb system. With annealing in vacuum at temperatures above $450\text{--}500^\circ\text{C}$, sublimation occurs not only for the crystalline Sb phase, but for the antimonides as well. This is reflected in the phase composition change by the following chemical reactions: $\text{CoSb}_2 \xrightarrow{600^\circ\text{C}} \text{Sb}\uparrow = \text{CoSb}$, $\text{CoSb}_3 \xrightarrow{600^\circ\text{C}} \text{Sb}\uparrow = \text{CoSb}_2$, $\text{CoSb}_3 + \text{Sb}\uparrow \xrightarrow{600^\circ\text{C}} \text{CoSb}_3$ and leads to increases in the amounts of the CoSb and CoSb_2 phases and decreases in the amounts of CoSb_3 . CoSb_x (30 nm) ($1.82 \leq x \leq 4.16$) films are found to be thermostable up to $\approx 350^\circ\text{C}$.

Keywords: skutterudite, phase, film, sublimation.

1. Introduction

Thermoelectricity, which is a priority in science and technology development, is based on the direct conversion of heat energy to electricity and vice versa. Skutterudite CoSb_3 has potential for use as a thermoelectric material [1-3]. Currently utilized thermoelectric materials have a maximum of efficiency ZT only in the range of 1 [4-5]. ZT is calculated by the formula $ZT = S^2 \sigma T / (k_{el} + k_L)$, where S is the Seebeck coefficient, σ is the electrical conductivity, T is the absolute temperature, k_{el} is the thermal conductivity from electrons, k_L is the thermal conductivity from lattice [2,6]. According to theoretical calculation, ZT increases with decreases in size and in nanomaterials, one can reach values ≥ 2 because of decreases in thermal conductivity from the lattice [7].

The aim of this work is to investigate the influence of deposition and thermal treatment conditions on the formation of phase composition and structure in nanoscaled CoSb_x (30 nm) ($1.82 \leq x \leq 4.16$) films on oxidized monocrystalline silicon.

2. Experimental procedure

30 nm thick CoSb_x ($1.82 \leq x \leq 4.16$) films were produced by molecular-beam epitaxy on a substrate of thermally oxidized (100 nm thick SiO_2) monocrystalline Si (001). Antimony was deposited at a constant rate of 0.3 \AA/s by an effusor heated to 470°C . Simultaneously, Co was codeposited by the electron-beam method. Phase composition modification was

accomplished by varying the Co deposition rate from 0.027 – 0.049 Å/s. The pressure in the work chamber was $9.3 \cdot 10^{-11}$ Pa. Substrate temperature was 200 °C. The Co content was determined by luminous flux in the molecular beam. The Co deposition rate was measured by an EIES (Electron Induced Emission Spectroscopy) optical system and was controlled by SENTINEL III Leybold system during deposition. The deposition process was thus regulated in order to maintain a film thickness of 30 nm.

The film composition was determined by Rutherford backscattering (RBS) with an accuracy of ± 1 at.% using He^+ -ions at an acceleration energy of 1.7 MeV.

The film thickness was determined by simulation of the RBS-spectra using the program “Simnra” for the handling of RBS-data. The statistical accuracy for the measurement of film thickness was ± 1 nm. This was confirmed by X-ray reflectometry. Samples were annealed in vacuum and under nitrogen from 300–700 °C for 0.5 – 5 hours. Chemical composition of films was determined by Rutherford backscattering spectrometry. Phase composition and structure were characterized by methods of X-ray diffraction (XRD) (Debye-Sherrer photomethod with photographic registration of x-ray beams and on diffractometer ULTIMA IV Rigaku with using $\text{Cu } k_\alpha$ radiation in Bragg-Brentano geometry). The XRD data were corrected by the Rachinger algorithm [8]. The films’ electroconductive properties were investigated by resistometry using the four-point method. The quantitative change of the phase composition in the films was determined metallographically by the intercept method on the photographs of the surface obtained by a scanning electron microscope. The relative error of this method is ≈ 4 %.

3. Results and discussion

Figure 1 presents the XRD patterns and photographs of the XRD patterns of the CoSb_x ($1.82 \leq x \leq 4.16$) films after deposition. Identification of the phase composition showed that in the $\text{CoSb}_{1.82}$ (64.5 at.% Sb) film, the antimonide of CoSb_2 was formed with a monoclinic crystal lattice (Fig. 1a). As follows from the photographs of XRD patterns, the films under investigation were polycrystalline without texture (Fig. 1b). Increased Sb content also resulted in the formation of polycrystalline skutterudite phase of CoSb_3 with a cubic lattice. This two-phase state is preserved in the films with up to 74.6 at.% Sb content. In this Sb content interval, the intensity ratio of the diffraction maxima of $I(210)\text{CoSb}_2/I(310)\text{CoSb}_3$ decreased, as is evidenced by the increase in CoSb_3 phase amount and decrease in CoSb_2 with increased Sb content (Fig. 2).

Fig. 3 represents the change of the films’ phase composition with increased Sb content in the interval from 64.5 to 74.6 at.%, according to the results of quantitative metallographic analysis of SEM-images. The single-phase structure is observed in both $\text{CoSb}_{1.82}$ and $\text{CoSb}_{2.89}$ films. In the $\text{CoSb}_{1.82}$ film, the CoSb_2 phase is formed and in the $\text{CoSb}_{2.89}$ film, the CoSb_3 phase is fixed. At intermediate compositions, these phases coexist. Meanwhile, with increased Sb content in films, the skutterudite CoSb_3 amount increases and the CoSb_2 phase amount decreases. Use of these two methods showed good correlation with the change of the phase composition in as-deposited films, subject to Sb content (Fig. 1 and Fig. 3).

In the as-deposited CoSb_x ($3.19 \leq x \leq 4.16$) films with higher Sb content, the two-phase composition was also observed. In addition to CoSb_3 in the films, the crystalline phase of Sb (Fig. 1) was also formed. From the change of ratio of diffraction peaks intensities of $I(012)\text{Sb}/I(310)\text{CoSb}_3$ it follows that with increased Sb content from 76.1 to 80.6 at.%, the amount of the crystalline Sb phase increases (Fig. 4).

The results of XRD structure and phase analysis of the films under investigation are presented in Table 1. It should be noted that in nanoscale films deposited at the substrate

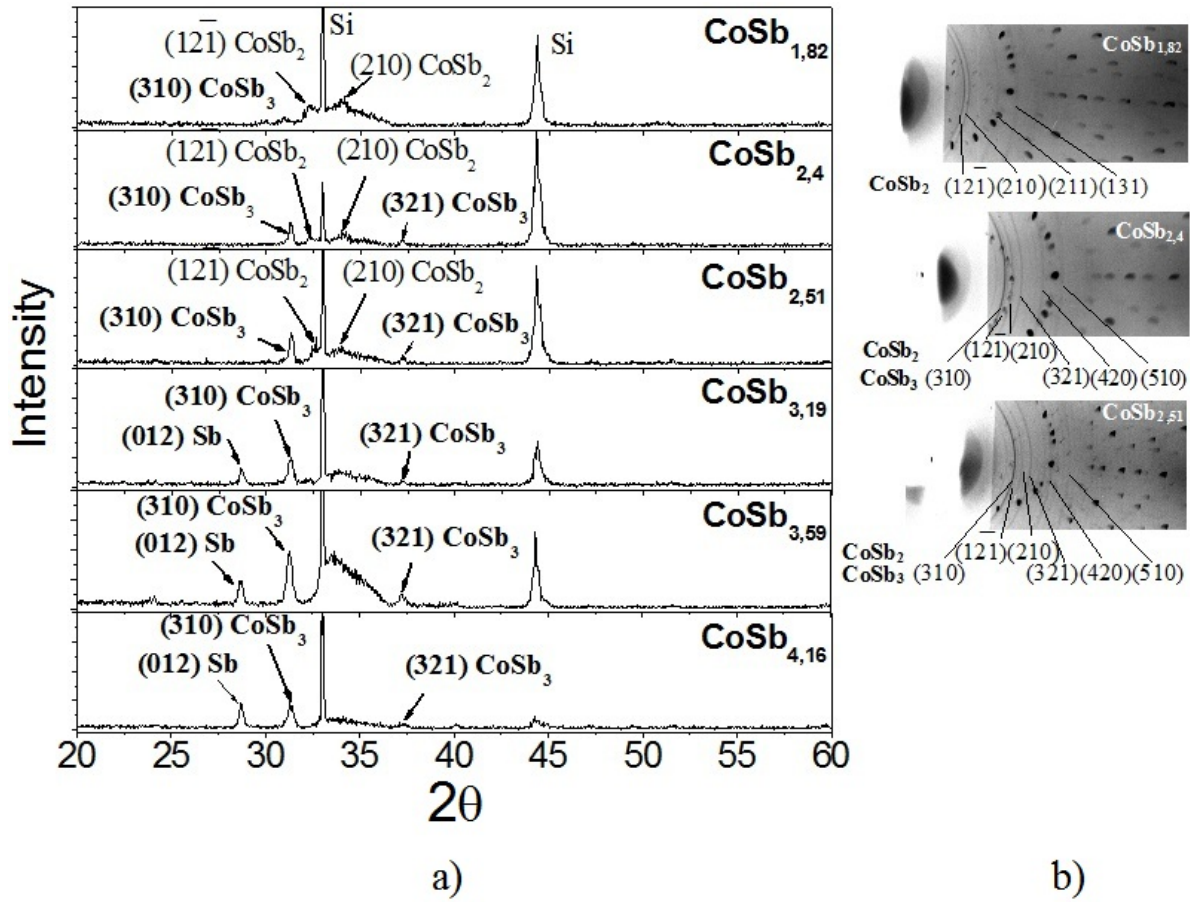


FIG. 1. XRD patterns (a) and photographs of XRD patterns (b) of the CoSb_x ($1.82 \leq x \leq 4.16$) films after deposition

temperature of 200°C good coincidence was observed for the phase composition with the phase diagram for bulk state.

TABLE 1. Phase composition of the as-deposited CoSb_x ($1.82 \leq x \leq 4.16$) films

| Substrate temperature, $^\circ\text{C}$ | Sb content in the film, at.% | | | |
|---|------------------------------|---------------------------------|-----------------------------------|-----------------------------|
| | 64.5 | 64.5–70 | 70–74.6 | 76.1–80.6 |
| | Ratio Sb/Co in the film | | | |
| | 1.82 | 1.82–2.3 | 2.3–2.89 | 3–4.16 |
| 200 | CoSb_2 | $\text{CoSb}_2 + \text{CoSb}_3$ | $\text{CoSb}_3 + (\text{CoSb}_2)$ | $\text{CoSb}_3 + \text{Sb}$ |

Annealing of CoSb_x ($2.4 \leq x \leq 2.89$) films in vacuum causes a change in their phase composition.

As follows from Figure 5, after annealing at 620°C , the ratio $I(210)\text{CoSb}_2/I(310)\text{CoSb}_3$ increases with a noted absence of texture. This indicated an increase in the CoSb_2 amount.

The as-deposited CoSb_x ($3.19 \leq x \leq 4.16$) films had a two-phase crystalline structure from a skutterudite phase of CoSb_3 and a crystalline Sb phase. From the change in the ratio of the diffraction peak intensities of $I(210)\text{CoSb}_2/I(310)\text{CoSb}_3$ after annealing in the Sb-enriched films of $\text{CoSb}_{3.59}$ and $\text{CoSb}_{4.16}$, it follows that with annealing under 500°C , phase changes don't occur (Fig. 6).

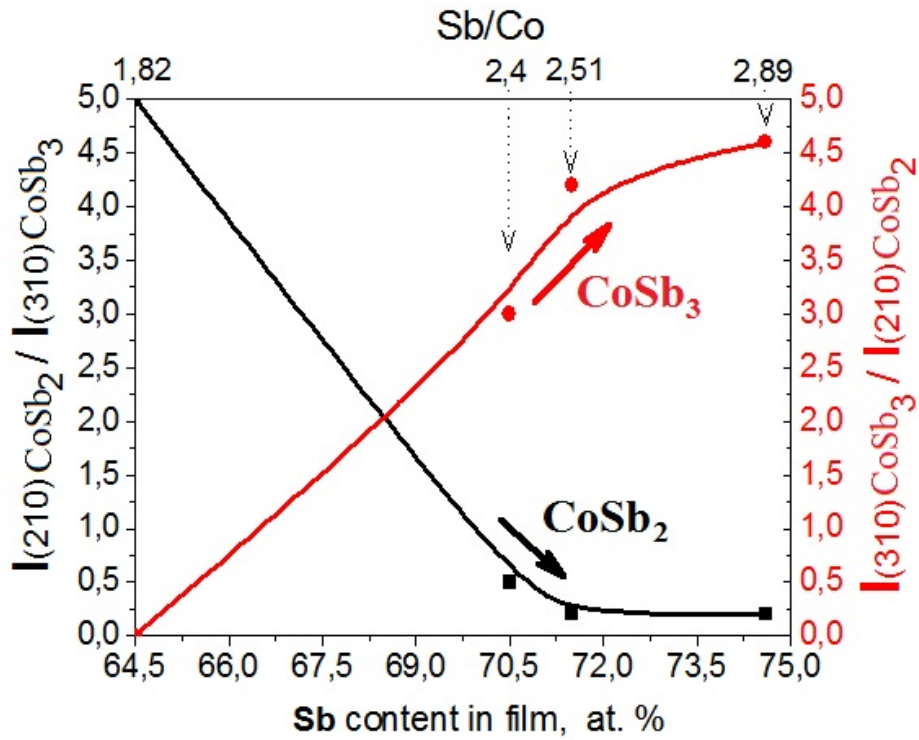


FIG. 2. XRD integral intensity ratio of $I(210)\text{CoSb}_2/I(310)\text{CoSb}_3$ and $I(310)\text{CoSb}_3/I(210)\text{CoSb}_2$ for the as-deposited CoSb_x ($1.82 \leq x \leq 2.89$) films

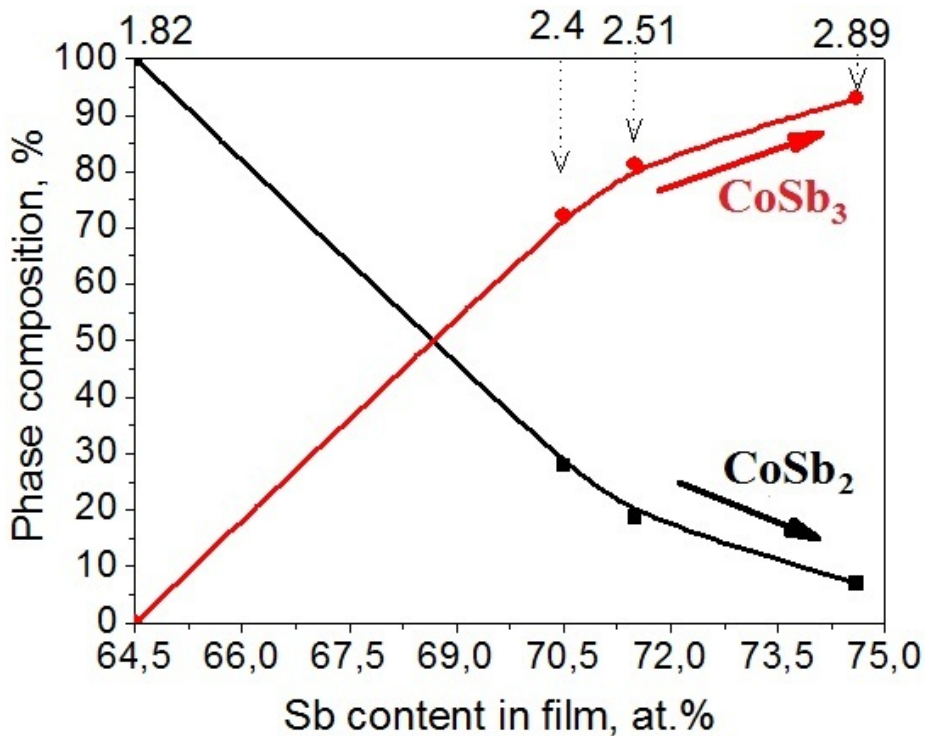


FIG. 3. Change of phase composition in the as-deposited CoSb_x ($1.82 \leq x \leq 2.89$) films

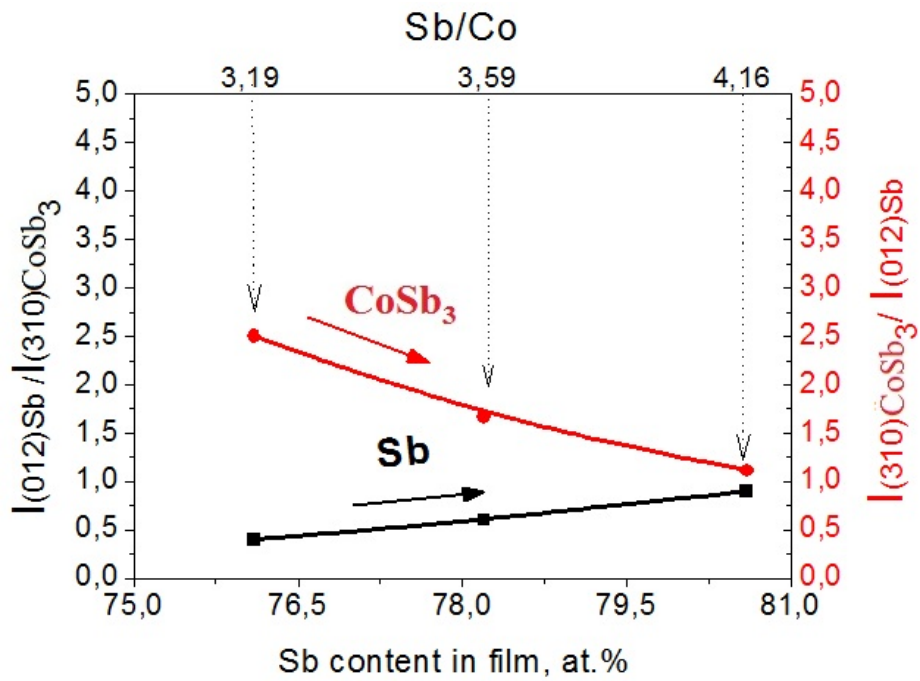


FIG. 4. XRD integral intensity ratio of $I(012)Sb/I(310)CoSb_3$ and $I(310)CoSb_3/I(012)Sb$ for the as-deposited $CoSb_x$ ($3.19 \leq x \leq 4.16$) films

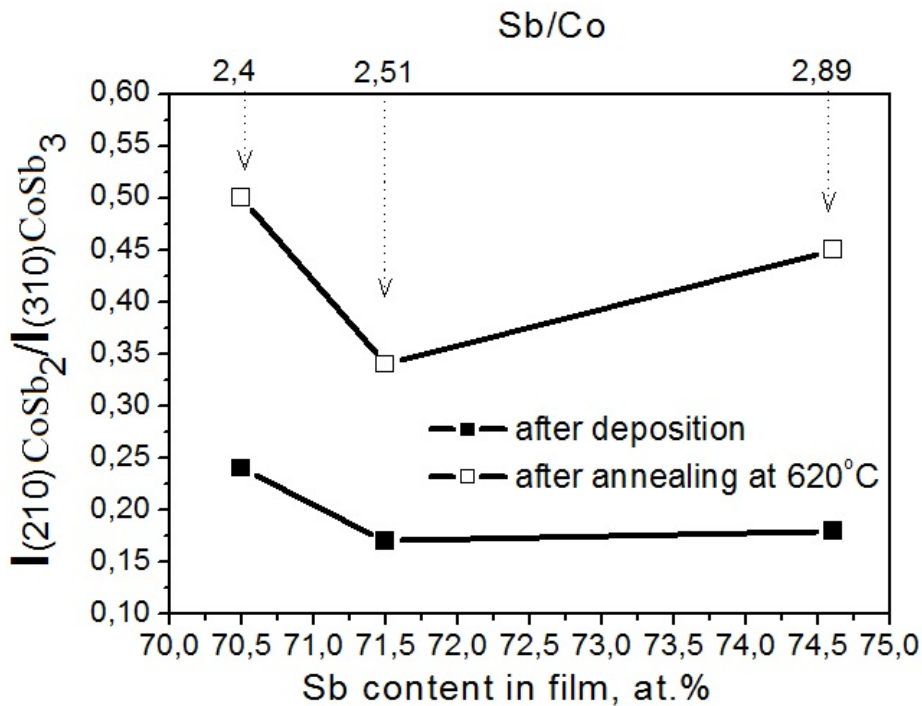


FIG. 5. XRD integral intensity ratio of $I(210)CoSb_2/I(310)CoSb_3$ for the $CoSb_x$ ($2.4 \leq x \leq 2.89$) films after deposition and annealing in vacuum at $620^\circ C$ for 30s

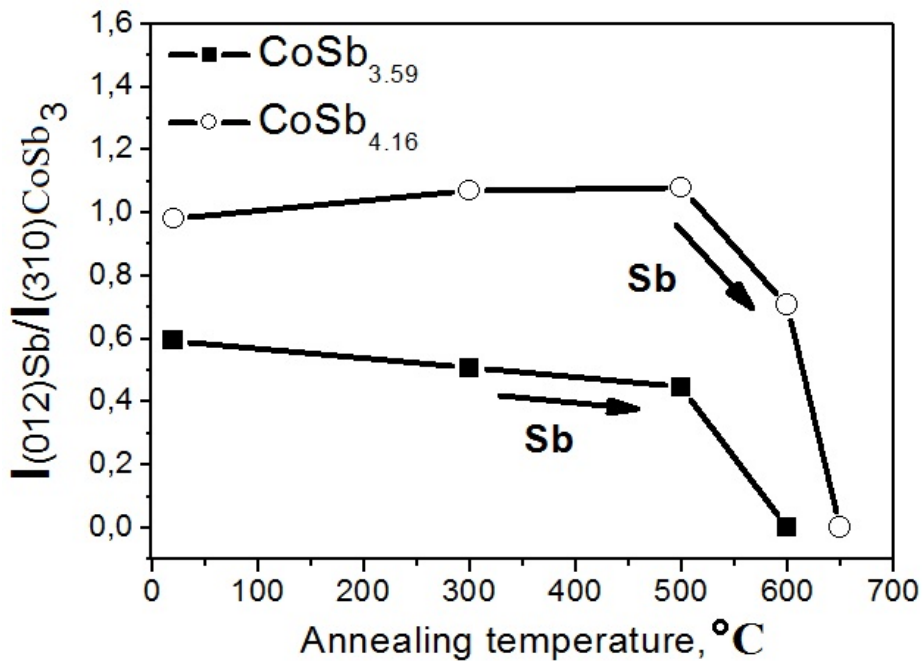


FIG. 6. XRD integral intensity ratio of $I(012)Sb/I(310)CoSb_3$ for the $CoSb_{3.59}$ and $CoSb_{4.16}$ films after annealing in vacuum at different temperatures

During annealing at higher temperatures, intense sublimation of Sb occurred. After annealing at $600^\circ C$, the reflexes of the crystalline Sb weren't observed and only the $CoSb_3$ phase remained.

Figure 7 shows the data for the quantitative analysis of the phase composition change in films having a two-phase composition of $(CoSb_3 + Sb)$ after annealing, determined using the ratio intensities of the diffraction lines for $(012)Sb$ and $(310)CoSb_3$ according to a previously reported method [9]. The process of Sb sublimation, also from antimonides, also holds for the annealing of bulk materials [10].

The process of Sb sublimation also occurs with annealing under nitrogen. According to XRD data for the structure and phase analysis in the as-deposited $CoSb_{1.82}$ film with lowest Sb content (64.5 at.% Sb), only the $CoSb_2$ phase was observed, and after annealing at $600^\circ C$, a two-phase state of $CoSb_2$ and Sb was formed. In the $CoSb_{2.4}$ and $CoSb_{2.51}$ films with Sb content of 70.5 and 71.5 at.% respectively, before and after such annealing, the two-phase composition was preserved for the antimonides of $CoSb_2$ and $CoSb_3$.

Figure 8 represents the data for the quantitative metallographic analysis of the SEM-images of the $CoSb_x$ ($1.82 \leq x \leq 2.51$) films after deposition and thermal treatment. After annealing a quantitative change of the phase composition was observed. In the film with Sb content of 64.5 at.% after annealing at $600^\circ C$, nearly 30% of the Sb phase appeared. In films with 70.5 and 71.5 at.% Sb content, the amount of the $CoSb_2$ phase increased and amount of the $CoSb_3$ skutterudite decreased.

This can be explained by the partial sublimation of Sb from the crystalline lattices of the $CoSb$ and $CoSb_3$ antimonides with annealing both in nitrogen and in vacuum due to the following chemical reactions: $CoSb_2 \xrightarrow{600^\circ C} Sb\uparrow = CoSb_2 + CoSb$; $CoSb_3 \xrightarrow{600^\circ C} Sb\uparrow = CoSb_3 + CoSb_2$.

Thermal stability of the nanoscale skutterudite films of $CoSb_x$ ($3.19 \leq x \leq 4.16$) was preserved up to $\approx 300-350^\circ C$ (Fig. 9).

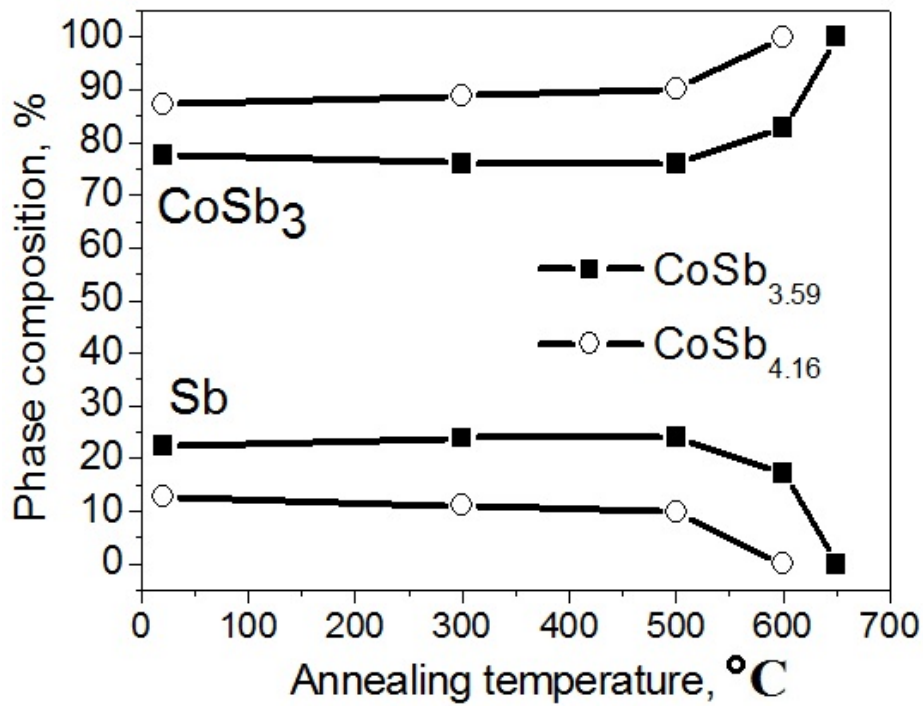


FIG. 7. Phase composition of the CoSb_{3.59} and CoSb_{4.16} films after annealing in vacuum at the different temperatures for 30s

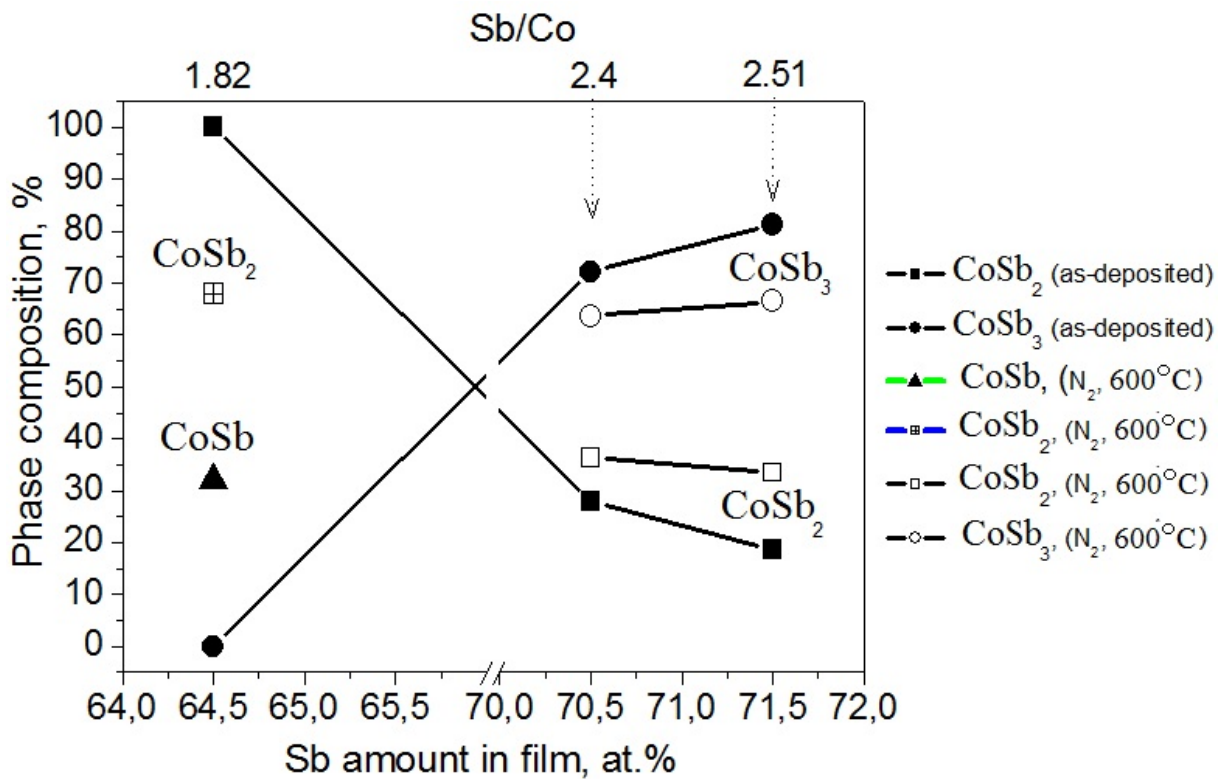


FIG. 8. Phase composition of the as-deposited films and the films post-annealed in nitrogen at 600 °C for 30s

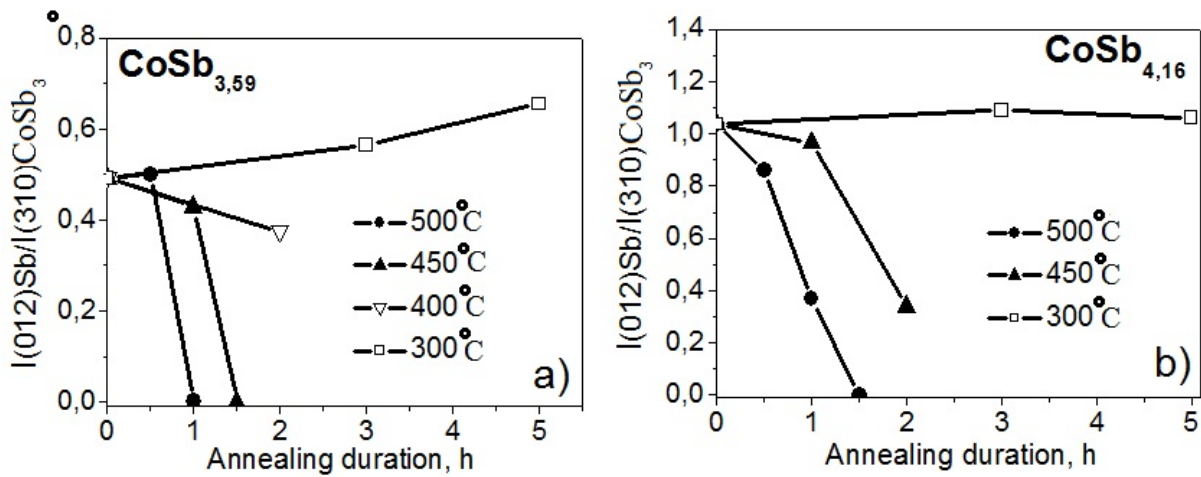


FIG. 9. Dependence of the ratio of the diffraction peaks intensities of $I(012)Sb/I(310)CoSb_3$ of the $CoSb_{3,59}$ (a) and $CoSb_{4,16}$ (b) films on annealing duration in vacuum at 300 °C, 400 °C, 450 °C, 500 °C

The activation energy for the Sb sublimation process was determined using the rate of the Sb sublimation at different annealing temperatures, according to the Arrhenius equality [10].

The sublimation process for crystalline Sb is dependent upon the chemical composition of the films (Fig. 10).

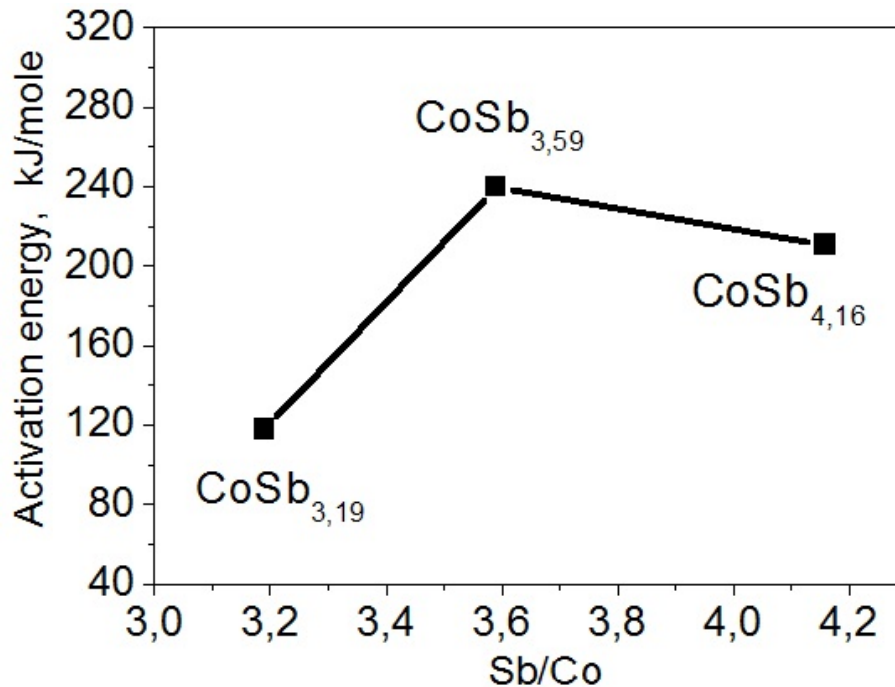


FIG. 10. Change of the activation energy of Sb sublimation in the $CoSb_x$ ($3.19 \leq x \leq 4.16$) films

The electrophysical properties of the Co-Sb films depended on their phase composition. The dependence of the resistivity of the as-deposited films on the Sb amount has

a parabolic character with a maximum of $15 \mu\Omega \cdot \text{cm}$ at the Sb concentration of 75 at.% (Fig. 11).

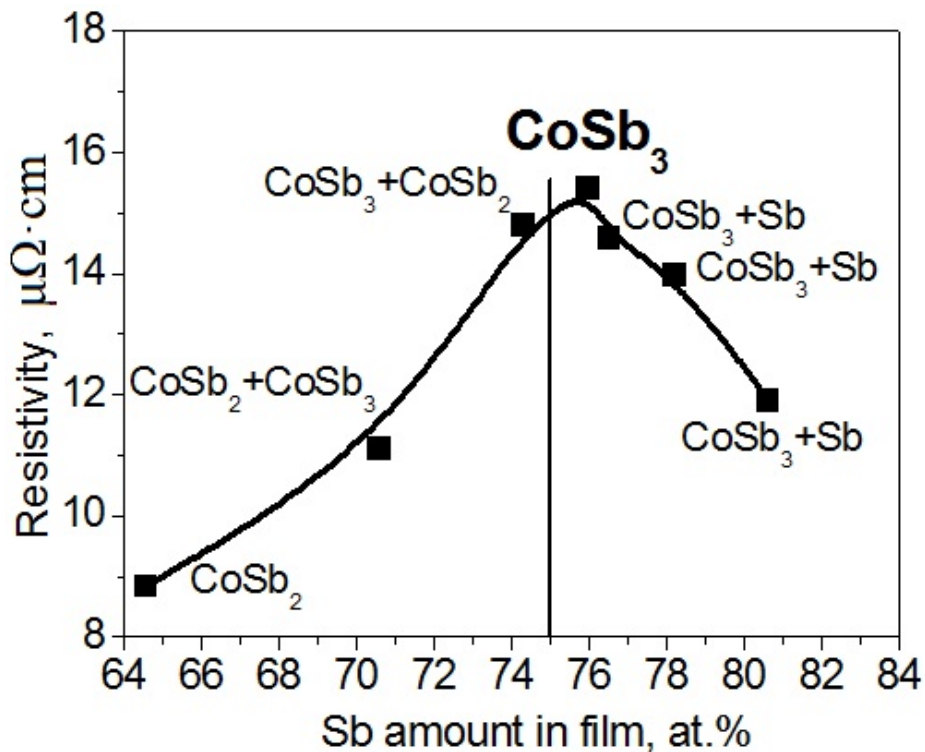


FIG. 11. Dependence of the resistivity of CoSb_x ($1.82 \leq x \leq 4.16$) on Sb amount

Skutterudite CoSb_3 is a semiconductor and has higher resistivity in comparison with phases of CoSb_2 and Sb having a semiconductor and metallic type of the conductivity respectively. The difference in the phase composition has influence not only on the absolute values of the film resistivity, but also on their temperature dependence. So, for the $\text{CoSb}_{2.98}$ and $\text{CoSb}_{3.055}$ films, in which the CoSb_3 phase was generally present, the dependence of the resistivity on the temperature has a semiconductor character (Fig. 12).

In the films having two-phase composition from CoSb_3 and Sb, the temperature dependence of the resistivity takes on a form typical for metals. According to report [8], Sb has a metallic type of conductivity.

4. Conclusion

It was established that at a substrate temperature of 200°C , during the deposition of CoSb_x ($1.82 \leq x \leq 4.16$) films, they were formed in a crystalline state. The films were in a polycrystalline state without texture. Good correlation between the film phase composition and the phase diagram for the bulk materials was observed. With increased Sb content, the formation of the phase composition occurs in same sequence as is provided by the phase diagram for bulk materials of the Co-Sb system.

In CoSb_x films, the phase formation sequence versus Sb amount is as follows:

- at 64.5 at.% Sb, the film formed is an antimonide of CoSb_2 ;
- from 64.5 to 75 at.% Sb, along with the CoSb_2 phase, the skutterudite of CoSb_3 was formed. CoSb_3 content increased with increased Sb;
- near 75 at.% Sb, the crystalline phase of CoSb_3 was formed;

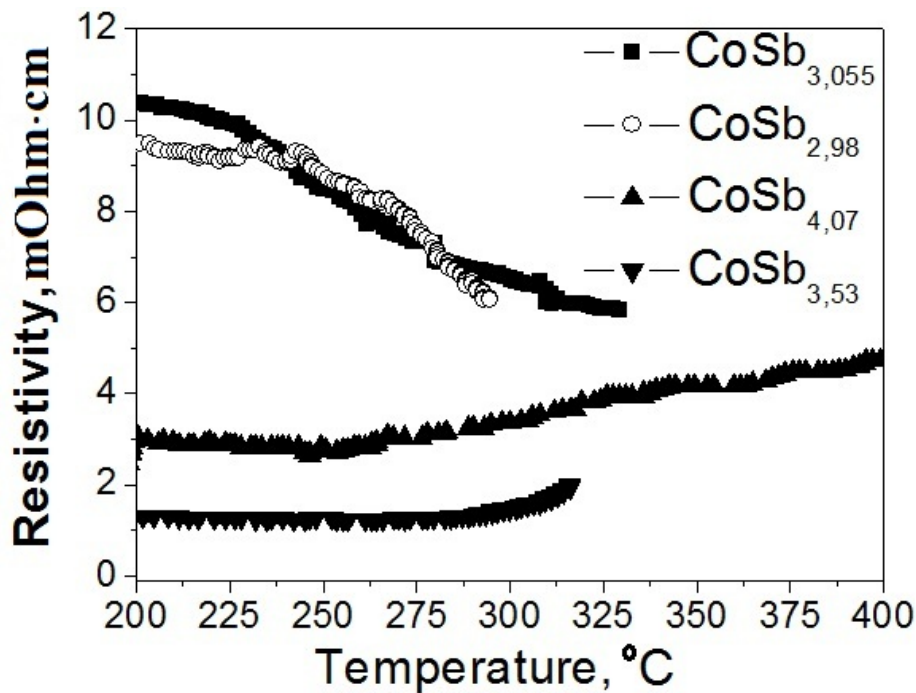


FIG. 12. Dependence of the resistivity of the CoSb_x ($2.98 \leq x \leq 4.07$) films on temperature

- at greater than 75 at.% Sb, in addition to CoSb_3 , the crystalline phase of Sb was formed;

With annealing in vacuum at temperatures higher than 450–500 °C, Sb sublimation occurred, which is reflected in the change of the phase composition according to the following chemical reactions: $\text{CoSb}_2 \xrightarrow{600^\circ\text{C}} \text{Sb}\uparrow = \text{CoSb}$, $\text{CoSb}_3 \xrightarrow{600^\circ\text{C}} \text{Sb}\uparrow = \text{CoSb}_2$. This resulted in an increase in the CoSb and CoSb_2 amount and a decrease in the CoSb_3 amount.

The CoSb_x ($1.82 \leq x \leq 4.16$) films were thermostable up to ≈ 350 °C.

Acknowledgments

The authors would like to thank Prof. M. Albrecht and Dr. G. Beddies, PhD. M. Daniel and workers from Chemnitz University of Technology (Germany) for sample preparation, assistance in conduction of investigations and discussion of results.

This work was financially supported by the Deutsche Akademischer Austauschdienst (DAAD) in the frame of the Leonard-Euler-Program (Grant N 50744282).

References

- [1] G.A. Slack, in CRC Handbook of Thermoelectrics, edited by D.M. Rowe (CRC, Boca Ration, 1995), p. 407.
- [2] Peng-Xian Lu, Qiu-Hua Ma, Yuan Li, Xing Hu. A study of electronic structure and lattice dynamics of CoSb_3 skutterudite. *Journal of Magnetism and Magnetic Materials*, **322**, P. 3080–3083 (2010).
- [3] Xu-qiu Yang, Peng-cheng Zhai, Li-sheng Liu, and Qing-jie Zhang. Thermodynamic and mechanical properties of crystalline CoSb_3 : A molecular dynamics simulation study. *Journal of Applied Physics*, **109**, P. 123517 (2011).
- [4] Ruiheng Liu, Xihong Chen, Pengfei Qiu, Jinfeng Liu, Jiong Yang, Xiangyang Huang, and Lidong Chen. Low thermal conductivity and enhanced thermoelectric performance of Gd-filled skutterudites. *Journal of Applied Physics*, **109**, P. 023719 (2011).

- [5] Jian-Li Mi, Mogens Christensen, Eiji Nishibori, and Bo Brummerstedt Iversen. Multitemperature crystal structures and physical properties of the partially filled thermoelectric skutterudites $M_{0.1}Co_4Sb_{12}$ ($M = La, Ce, Nd, Sm, Yb, \text{ and } Eu$). *Physical Review B* **84**, P. 064114 (2011).
- [6] Jianjun Zhang, Bo Xu, Li-Min Wang. Great thermoelectric power factor enhancement of $CoSb_3$ through the lightest metal element filling. *Applied physics letters*, **98** P. 072109 (2011).
- [7] M. Wilczyski. Thermopower, figure of merit and spin-transfer torque induced by the temperature gradient in planar tunnel junctions. *J. Phys.: Condens. Matter*, **23**, P. 456001 (2011).
- [8] M. Daniel, M. Friedemann, N. Jöhrmann, A. Liebig, J. Donges, M. Hietschold, G. Beddies, M. Albrecht. Influence of the substrate thermal expansion coefficient on the morphology and elastic stress of $CoSb_3$ thin films. *Phys. Status Solidi A*, **210**(1), P. 140–146 (2013).
- [9] A.A. Rusakov. *Rentgenografiya metallov*. Uchebnic dlya vusov. M., Atomizdat (1977), P. 389–407.
- [10] Degang Zhaoa, Changwen Tiana, Yunteng Liua. High temperature sublimation behavior of antimony in $CoSb_3$ thermoelectric material during thermal duration test. *Journal of Alloys and Compounds*. **509**, P. 3166–3171 (2011).